

MEASUREMENT OF A PEAK IN THE COSMIC MICROWAVE BACKGROUND POWER SPECTRUM FROM THE NORTH AMERICAN TEST FLIGHT OF BOOMERANG

P.D. MAUSKOPF¹, P.A.R. ADE², P. DE BERNARDIS³, J.J. BOCK^{4,5}, J. BORRILL^{6,7}, A. BOSCALERI⁸, B.P. CRILL⁴, G. DEGASPERIS⁹, G. DE TROIA³, P. FARESE¹⁰, P. G. FERREIRA^{11,12}, K. GANGA^{13,14}, M. GIACOMETTI³, S. HANANY¹⁵, V.V. HRISTOV⁴, A. IACOANGELI³, A. H. JAFFE⁶, A.E. LANGE⁴, A. T. LEE¹⁶, S. MASI³, A. MELCHIORRI¹⁷, F. MELCHIORRI³, L. MIGLIO³, T. MONTROY¹⁰, C.B. NETTERFIELD¹⁸, E. PASCALE⁸, F. PIACENTINI³, P. L. RICHARDS¹⁶, G. ROMEO¹⁹, J.E. RUHL¹⁰, E. SCANNAPIECO¹⁶, F. SCARAMUZZI²⁰, R. STOMPOR¹⁶ AND N. VITTORIO⁹

¹ Dept. of Physics and Astronomy, University of Massachusetts, Amherst, MA, USA

² Queen Mary and Westfield College, London, UK

³ Dipartimento di Fisica, Università La Sapienza, Roma, Italy

⁴ California Institute of Technology, Pasadena, CA, USA

⁵ Jet Propulsion Laboratory, Pasadena, CA, USA

⁶ Center for Particle Astrophysics, University of California, Berkeley, CA, USA

⁷ National Energy Research Scientific Computing Center, LBNL, Berkeley, CA, USA

⁸ IROE-CNR, Firenze, Italy

⁹ Dipartimento di Fisica, Università di Roma Tor Vergata, Roma, Italy

¹⁰ Dept. of Physics, Univ. of California, Santa Barbara, CA, USA

¹¹ CENTRA, IST, Lisbon, Portugal

¹² Theory Division, CERN, Geneva, Switzerland

¹³ Physique Corpusculaire et Cosmologie, Collège de France, 11 Place Marcelin Berthelot, 75231 Paris Cedex 05, France

¹⁴ IPAC, Pasadena, CA, USA

¹⁵ Dept. of Physics, University of Minnesota, Minneapolis, MN, USA

¹⁶ Dept. of Physics, University of California, Berkeley, CA, USA

¹⁷ Dept. de Physique Théorique, Université de Genève, Switzerland

¹⁸ Depts. of Physics and Astronomy, University of Toronto, Canada

¹⁹ Istituto Nazionale di Geofisica, Roma, Italy

²⁰ ENEA, Frascati, Italy

ABSTRACT

We describe a measurement of the angular power spectrum of anisotropies in the Cosmic Microwave Background (CMB) from 0.3° to $\sim 10^\circ$ from the North American test flight of the BOOMERANG experiment. BOOMERANG is a balloon-borne telescope with a bolometric receiver designed to map CMB anisotropies on a Long Duration Balloon flight. During a 6-hour test flight of a prototype system in 1997, we mapped > 200 square degrees at high galactic latitudes in two bands centered at 90 and 150 GHz with a resolution of 26 and 16.6 arcmin FWHM respectively. Analysis of the maps gives a power spectrum with a peak at angular scales of ~ 1 degree with an amplitude $\sim 70\mu K_{CMB}$.

Subject headings: cosmology: Cosmic Microwave Background, anisotropy, measurements, power spectrum

1. INTRODUCTION

Measurements of Cosmic Microwave Background (CMB) anisotropies have the potential to reveal many of the fundamental properties of the universe (e.g. see Kamionkowski & Kosowsky 1999 and references therein). Since the measurement of the large scale anisotropies by COBE-DMR (Wright et al. 1994, Bennett et al. 1996, etc.), many ground-based and balloon-borne experiments have continued to develop the technology necessary to produce accurate measurements of CMB structure on smaller angular scales. Recent results from these experiments have shown evidence for the existence of a peak in the power spectrum of CMB fluctuations at a multipole, $\ell \sim 200$ (Netterfield et al. 1997, de Oliveira-Costa et al. 1998, Wilson et al. 1999, Torbet et al. 1999, Coble et al. 1999, Miller et al. 1999). In this paper, we present results from the test flight of BOOMERANG that constrain the position and amplitude of this peak. In fact, the results from this data set alone can be used to constrain cosmological models and provide evidence for a flat universe, $\Omega = \Omega_M + \Omega_\Lambda \simeq 1$ (see the companion paper, Melchiorri,

et al. 1999).

BOOMERANG is a millimeter-wave telescope and receiver system designed for a Long Duration Balloon (LDB) flight from Antarctica of up to two weeks duration. The data presented here are from a prerequisite test flight of the payload in August, 1997, which lasted 6 hours at float altitude. A prototype of the LDB focal plane was used to test the experimental strategy of making a map and measuring the angular power spectrum of CMB anisotropy with a slowly-scanned telescope and total-power bolometric receiver.

2. INSTRUMENTATION

BOOMERANG employs bolometric detectors cooled to 0.3 K, coupled to an off-axis telescope and operated as total power radiometers. Electronic modulation and synchronous demodulation of the bolometer signals provide low frequency stability of the detector system. The optical signal is modulated by slowly scanning the telescope (~ 1 deg/s) in azimuth. A description of the instrument can be found in Masi et al. 1999a.

The BOOMERANG telescope consists of three off-axis, aluminum mirrors: an ambient temperature 1.3 m primary mirror and two smaller (15 cm) 2 K reimaging mirrors. The telescope is shielded from ground radiation by extensive low emissivity baffles. Incoming radiation is reflected by the primary mirror into the entrance window of the cryostat and reimaged by the 2 K optics onto the 0.3 K focal plane. The tertiary mirror is positioned at an image of the primary mirror and forms a throughput-limiting Lyot stop illuminating the central 85 cm of the primary mirror. The inside of the 2 K optics box has a thick coating of absorbing material (Bock 1994) to intercept stray light. A calibration lamp mounted in the Lyot stop of the optical system is pulsed for ~ 0.5 s every 15 minutes to produce a stable, high signal-to-noise ratio ($\gtrsim 1000$) calibration transfer.

For the test flight, the focal plane contained silicon nitride micromesh bolometers (Mauskopf et al. 1997, Bock et al. 1998) fed by multi-mode feed horns with channels at 90 and 150 GHz. Fourier transform spectroscopy of each channel determined the average band centers and effective band widths for sources with a spectrum of CMB anisotropy (Table 1). A long duration ^3He cryostat (Masi et al. 1998, Masi et al. 1999b) maintained the focal plane at 0.285 ± 0.005 K during the flight. The bolometers were biased with an AC current and the signals were demodulated, amplified and passed through a 4-pole Butterworth low-pass filter with a cut-off frequency of 20 Hz for the 150 GHz channels and 10 Hz for the 90 GHz channels. The bolometer DC levels were removed with a single-pole, high-pass filter with a cut-on frequency of 16 mHz and re-amplified before digital sampling at 62.5 Hz with 16 bit resolution.

The attitude control system included a low-noise two-axis flux-gate magnetometer, a CCD star camera and three orthogonal (azimuth, pitch, roll) rate gyroscopes. The azimuth gyroscope drove the azimuth feedback loop, which actuated two torque motors, one of which drove a flywheel while the other transferred angular momentum to the balloon flight line. The gyroscope was referenced every scan to the magnetometer azimuth to remove long time scale drifts. Pendulations of the payload were reduced by a oil-filled damper mounted near the main bearing and sensed by the pitch and roll gyroscopes outside of the control loop. The CCD frame had 480×512 pixels, with a resolution of 0.81 arcmin/pixel (azimuth) and 0.65 arcmin/pixel (elevation). The limiting magnitude of stars used for pointing reconstruction was $m_V \sim 5$. The coordinates of the two brightest stars in each CCD frame were identified by on-board software and recorded at 5 Hz, for post-flight attitude reconstruction.

The primary mirror and the receiver were mounted on an inner frame which could be rotated to position the elevation boresight of the telescope between 35° – 55° . During observations, the inner frame was held fixed while the entire gondola slowly scanned in azimuth. The scan speed was set to the maximum allowed by the beam size and bolometer time constants. The window functions for the 90 and 150 GHz channels in this flight were rolled off at $\ell \gtrsim 300$ and 500, respectively, by the 26 and 16.5 arcmin beams and were limited to $\ell \gtrsim 20$ by the system $1/f$ noise.

3. OBSERVATIONS

The instrument was launched at 00:25 GMT on August 30, 1997 from the National Scientific Balloon Facility in Palestine, Texas. Observations started at 3:50 GMT and continued until the flight was terminated at 9:50 GMT. Sunset was at 01:00 GMT and the moon rose at 10:42 GMT. The average altitude at float was 38.5 km. We observed in three modes: ~ 4.5 hours of CMB scans, 40 minutes of calibration scans on Jupiter, and four ten-minute periods of full-sky rotations of the gondola. The CMB observations consisted of smoothed triangle wave scans in azimuth with a peak-to-peak amplitude of 40 degrees centered on due South at an elevation angle of 45 degrees. The scan rate was ~ 2.1 deg/s in azimuth (1.4 deg/s on the sky) in the linear portion of the scan (63% of the period). These scans, combined with the earth's rotation, covered a wide strip of sky, from $-73^\circ < \text{RA} < 23^\circ$ and $-20^\circ < \text{DEC} < -16^\circ$.

4. DATA REDUCTION

We obtain a first order reconstruction of the attitude from the elevation encoder and magnetometer data. Using this, the stars recorded by the CCD camera are identified. The data from the gyroscopes are used to interpolate between star identifications. The offset between the microwave telescope and the star camera is measured from the observation of Jupiter. The attitude solution obtained in this way is accurate to ~ 1 arcmin rms.

The results presented in this paper are primarily from the highest sensitivity 150 GHz channel. Data from a 90 GHz channel are presented as a systematic check. The data at float consist of ~ 1.4 million samples for each bolometer. These data are searched for large ($> 5\sigma$) deviations such as cosmic ray events and radio frequency interference and flagged accordingly. Flags are also set for events in the auxiliary data such as calibration lamp signals and elevation changes, as well as for the different scan modes. Unflagged data, used for the CMB analysis, are 54% of the total at 150 GHz and 60% of the total at 90 GHz. We deconvolve the transfer functions of the read-out electronics and the bolometer thermal response from the data, and apply a flat phase numeric filter to reduce high frequency noise and slow drifts. The time constants of the bolometers given in Table 1 are measured in flight from the response to cosmic rays and to fast (18 deg/s) scans over Jupiter.

Table 1. BOOMERANG 1997 instrument parameters

ν_0 (GHz)	$\Delta\nu$ (GHz)	FWHM (')	Ω 10^{-5} sr	τ_b (ms)	NET _{CMB} ($\mu\text{K}/\sqrt{\text{Hz}}$)
96	33	26	6.47 ± 0.27	71 ± 8	400
153	42	16.5	2.63 ± 0.10	83 ± 12	250

The primary calibration is obtained from scans of the telescope over Jupiter, which were performed from 3:32 U.T. to 3:53 U.T. (1.2 deg/s azimuth scans). Jupiter was also re-observed later during regular CMB scans (from 5:58 to 6:18 U.T.) and during full sky rotations. Jupiter was rising during the first observation (from an elevation of 36.9° to 38.2°) and setting during the second one (from an elevation of 40.1° to 39.0°). The deconvolved and filtered data from these scans are triangle-interpolated on a regular grid centered on the optical position of Jupiter to

make a beam map. The beams are symmetric with minor and major axes equivalent within 5%. Solid angles given in Table 1 are computed by integration of the interpolated data. The beam map is used to derive the window function, W_ℓ , and an overall normalization.

We use a brightness temperature of $T_{\text{eff}} = 173$ K for both the 90 and 150 GHz bands (Ulich 1981, Griffin 1986, Hildebrand 1985) and assume an uncertainty of 5% (Goldin et al. 1997). We also assign a 5% error in the conversion from brightness temperature to CMB temperature due to statistical noise in the measurements of the band pass. Errors in the determination of the receiver transfer function are largest at the highest temporal frequencies where signals are attenuated by the bolometer time constants. These errors affect the calibration of the window function and the CMB power spectrum measurements at the largest multipoles. These should cancel because the beam maps of Jupiter are made from scans at the same scan speed as the CMB scans. In simulations, a 15% error in the determination of the bolometer time constant produces a maximum error $< 1.5\%$ in the normalization and $\lesssim 6\%$ in the value of W_ℓ at $\ell < 300$ near scan turnarounds where the scan speed was only 1 deg/s. The final precision of the calibration including errors in the temperature of Jupiter, T_{eff} , the transfer function used for deconvolution, the measurement of the filter pass bands and the beam solid angle is 8.1% and 8.5% at 150 GHz and 90 GHz, respectively.

Signals from the internal calibration lamp are used to correct for a slow linear drift in detector responsivity during the flight, mainly due to variation (0.29-0.28 K) in the base temperature of the fridge. The change in response to the calibration lamp from the beginning to the end of the flight is +9%, -1% at 90 GHz, and +8%, -1.5% at 150 GHz.

5. MAP MAKING AND POWER SPECTRUM ESTIMATES

Current and future CMB missions require new methods of analysis able to incorporate the effects of correlated instrument noise and new implementations capable of processing large data sets (Bond et al. 1999). The analysis of the BOOMERANG test flight data provides a test of these methods on a moderate size ($\sim 25,000$ pixels) data set. The calibrated time stream data are processed to produce a pixelized map, and from this a measurement of the angular power spectrum, using the MADCAP software package of Borrill (1999a, 1999b) (see <http://cfpa.berkeley.edu/~borrill/cmb/madcap.html>) on the Cray T3E-900 at NERSC and the Cray T3E-1200 at CINECA.

Noise correlation functions are estimated from the time stream under the assumption that in this domain the signal is small compared to the noise. For the 150 GHz channel, the maximum likelihood map with 23,561, 1/3-beam sized (6.9') pixels is calculated from the noise correlation function, the bolometer signal (excluding flagged data and all data within 2 degrees of Jupiter) and the pointing information using the procedures described in Wright (1996), Tegmark (1997) and Ferreira & Jaffe (1999). The maximum likelihood power spectrum is estimated from the map using a Newton-Raphson iterative maximization of the C_ℓ likelihood function following Bond, Jaffe & Knox (1998) (BJK98) and Tegmark (1998). The power spectrum analy-

sis requires approximately 12 hours on sixty-four T3E-900 processors.

TABLE 2: ORTHOGONALIZED POWER SPECTRUM MEASUREMENT FROM BOOMERANG/NA150 GHz CHANNEL MAP WITH WITH 6 ARC-MINUTE PIXELS.

ℓ_{eff}	$[\ell_{\text{min}}, \ell_{\text{max}}]$	ΔT (μK) ^a	$\ell(\ell+1)C_\ell/2\pi$ (μK^2) ^b
58	[25, 75]	29^{+13}_{-11}	850^{+900}_{-540} (± 660)
102	[76, 125]	49^{+9}_{-9}	2380^{+990}_{-780} (± 860)
153	[126, 175]	67^{+10}_{-9}	4510^{+1380}_{-1140} (± 1250)
204	[176, 225]	72^{+10}_{-10}	5170^{+1500}_{-1320} (± 1410)
255	[226, 275]	61^{+11}_{-12}	3700^{+1500}_{-1300} (± 1390)
305	[276, 325]	55^{+14}_{-15}	3070^{+1680}_{-1530} (± 1570)
403	[326, 475]	32^{+13}_{-22}	1030^{+1020}_{-900} (± 1180)
729	[476, 1125]	< 130	250^{+16500}_{-250} (± 2710)

^a Errors from 68% confidence intervals

^b Errors from 68% confidence intervals with $\pm 1\sigma$ assuming Gaussian likelihood function in parentheses

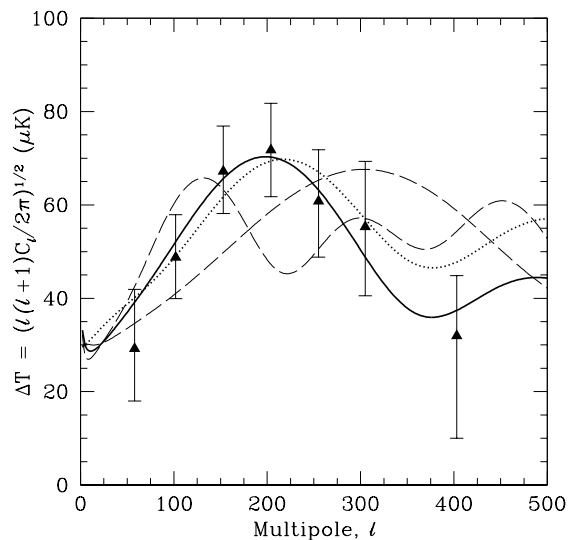


FIG. 1.— Power spectrum of the BOOMERANG 150 GHz map with 6 arcminute pixelization. The solid curve is a marginally closed model with $(\Omega_b, \Omega_M, \Omega_\Lambda, n_S, h) = (0.05, 0.26, 0.75, 0.95, 0.7)$. The dotted curve is standard CDM with $(0.05, 0.95, 0.0, 1.0, 0.65)$. Dashed curves are open and closed models with fixed $\Omega_{\text{total}} = 0.66$ and 1.55, respectively (see the companion paper, A. Melchiorri, et al. 1999).

Due to finite sky coverage, individual C_ℓ values are not independent, and we estimate the power in eight bins over $25 < \ell < 1125$, binning more finely at low ℓ than high. In each bin we calculate the maximum likelihood amplitude of a flat power spectrum in that bin, i.e. $\ell(\ell+1)C_\ell = \text{constant}$ (Table 2). Given our insensitivity to low ℓ signal, and in order to ameliorate the effects of low-frequency noise (which translates into low- ℓ structure for this scanning strategy), we marginalize over power at $\ell < 25$ and diagonalize the bin correlation matrix using a variant of techniques discussed in BJK98. Bin to bin signal correlations are small but non-negligible, with each top-hat bin anticorrelated with its nearest neighbors at approximately the 10% level.

We calculate likelihood functions for each bin using the offset log-normal distribution model of BJK98. We quote

errors for the power spectrum from $\pm 1\sigma$ errors assuming simple Gaussian likelihood functions and from 68% confidence intervals for the full likelihood functions. Plots of the likelihood functions are presented in the companion paper (Melchiorri, et al. 1999) and full spectral data including information on the shape of the likelihood function (Bond, Jaffe & Knox 1998b) and appropriate window and filter functions (Knox 1999) will be available at the BOOMERANG web site (<http://boom.physics.ucsb.edu> or <http://oberon.roma1.infn.it/boom>). In Figure 1, we show the calculated power spectrum for the 150 GHz channel 6 arcminute pixel map.

6. SYSTEMATICS CHECKS AND FOREGROUNDS

The scan strategy and analysis allow for a variety of checks for systematic effects in the data. For all systematic tests we produce small (~ 4000 pixel) maps with $16'$ pixels which can be generated and analyzed quickly (~ 30 minutes on four T3E-900 processors). Monte-Carlo simulations show the effects of the $16'$ pixelization are negligible for values of $\ell < 400$. Compared to the level of statistical noise, we find that the derived power spectrum from the 150 GHz channel is insensitive to (i) the size of the excluded region around Jupiter, (ii) the choice of spectral shape within the multipole bins, and (iii) the method of marginalizing over low ℓ signals.

We also analyze maps made from combinations of data that we expect to produce null power spectra in the absence of spurious sources of noise power: (i) data from a dark detector and (ii) the difference between left and right-going scans at 150 GHz. In each case (Table 3), we find a power spectrum consistent with zero.

Table 3. Power Spectra, $\ell(\ell+1)C_\ell/2\pi$, from BOOMERANG systematic tests. Error bars are $\pm 1\sigma$, assuming Gaussian likelihood functions. Unlike the data in Table 2 and Figure 1, these spectra are calculated with 16 arcminute pixels and have not been orthogonalized. The (L-R) difference analysis in column 5 has not been corrected for the effects of correlated noise, which leads to negative power estimates in the high ℓ bins.

$[\ell_{\min}, \ell_{\max}]$	150 GHz ($\mu\text{K}^2/100$)	90 GHz ($\mu\text{K}^2/100$)	Dark ($\mu\text{K}^2/100$)	150 (L-R)/2 ($\mu\text{K}^2/100$)
[25, 75]	10 ± 7	16 ± 12	-1 ± 1	4 ± 7
[76, 125]	23 ± 9	25 ± 13	1 ± 1	-9 ± 4
[126, 175]	46 ± 13	50 ± 20	1 ± 2	-7 ± 9
[176, 225]	50 ± 14	53 ± 25	6 ± 4	12 ± 17
[226, 275]	29 ± 13	21 ± 29	-1 ± 5	-22 ± 18
[276, 325]	23 ± 15	5 ± 40	2 ± 7	-30 ± 26
[326, 475]	8 ± 12	3 ± 48	7 ± 5	-78 ± 21
[476, 1125]	2 ± 27	2 ± 253	9 ± 12	-169 ± 52
[25, 475]	31 ± 5	25 ± 7	-1 ± 1	-4 ± 2

The sky strip observed is extended in Galactic latitude from $b \sim 15^\circ$ to $b \sim 80^\circ$. From IRAS/DIRBE map extrapolation (Schlegel et al. 1998) dust emission is not expected to produce significant contamination in this region of the sky. We find an amplitude for a flat power spectrum from $25 < \ell < 400$ of $\ell(\ell+1)C_\ell/2\pi = (3580 \pm 706)\mu\text{K}^2$ and $(2982 \pm 702)\mu\text{K}^2$ from the half of the map near the

galactic plane ($15^\circ < b < 45^\circ$) and the higher-latitude half ($45^\circ < b < 80^\circ$), respectively. Because of sky rotation, this also corresponds to separately analyzing the data from the first half and second half of the flight.

Jupiter is more than 1000 times brighter than degree-scale anisotropy in the CMB and is in the middle of the lowest latitude half of the map. We test for sidelobe contamination by varying the size of the circular avoidance zone around Jupiter from $\phi = 0.5 - 3$ degrees for the CMB maps, and find no significant change in the power spectrum as long as we remove data within ~ 1 degree.

7. DISCUSSION AND CONCLUSIONS

Data obtained in ~ 4.5 hours of CMB scans during the BOOMERANG test flight have been analyzed to produce maps of the millimeter-wave sky at 90 and 150 GHz, with 26 and 16 arcmin FWHM resolution, respectively. The instrument was calibrated using observations of Jupiter. The experiment employed a new scan strategy and detector technology designed to give maximum coverage of angular scales. The data analysis implements new techniques for making maximum likelihood maps from low signal-to-noise time stream data over large numbers of pixels. The power spectrum C_ℓ obtained from the maps extends from $\ell \sim 50$ to $\ell \sim 800$ and shows a peak at $\ell \sim 200$.

Since the BOOMERANG/NAtest flight in August, 1997, we have obtained > 200 hours of data from the LDB flight of BOOMERANG (BOOMERANG /LDB), carried out in Antarctica at the end of 1998. The focal plane for the LDB flight contained 2, 6, and 3 detectors at 90, 150, and 240 GHz, each with better sensitivity to CMB, faster time constants, and lower $1/f$ noise than the best channel in the BOOMERANG/NAflight, as well as 3 detectors at 400 GHz to provide a monitor of interstellar dust and atmospheric emission. The results from this flight will be reported elsewhere.

We thank the staff of the NASA NSBF for their excellent support of the test flight. We are also grateful for the help and support of a large group of students and scientists (a list of contributors to the BOOMERANG experiment can be found at <http://astro.caltech.edu/~bpc/boom98.html>). The BOOMERANG program has been supported by Programma Nazionale Ricerche in Antartide, Agenzia Spaziale Italiana and University of Rome La Sapienza in Italy; by NASA grant numbers NAG5-4081, NAG5-4455, NAG5-6552, NAG53941, by the NSF Science & Technology Center for Particle Astrophysics grant number SA1477-22311NM under AST-9120005, by NSF grant 9872979, and by the NSF Office of Polar Programs grant number OPP-9729121 in the USA; and by PPARC in UK. This research also used resources of the National Energy Research Scientific Computing Center, which is supported by the Office of Science of the U.S. Department of Energy under Contract No. DE-AC03-76SF00098. Additional computational support for the data analysis has been provided by CINECA/Bologna.

REFERENCES

- Bennett, C. L. et al. 1996, ApJ, 464, 1
- Bock, J. J., et al. 1998, ESA proceedings
- Bock, J. J. 1994, PhD. Thesis, Berkeley, CA
- Bond, J. R., Jaffe A. H., & Knox L. 1998, Phys. Rev. D, 57, 2117
- Bond, J. R., Jaffe, A. H., & Knox, L. 1998, ApJ, in press, astro-ph/9808264
- Bond D., Crittenden, Jaffe A., Knox L., 1999, Computing in Science and Engineering, 1, 21, astro-ph/9811148
- Borrill, J. 1999b, *The Challenge of Data Analysis for Future CMB Observations*, in "Proceedings of the 3K Cosmology: EC-TMR Conference", Rome, Italy edited by L. Maiani, F. Melchiorri, and N.Vittorio AIP Conference Proceedings, astro-ph/9903204
- Borrill, J. 1999b, *MADCAP: The Microwave Anisotropy Dataset Computation Analysis Package*, in "Proceedings of the Fifth European SGI/Cray MPP Workshop"
- Borrill, J. 1999a, Phys Rev D, 59, 7302, astro-ph/9712121
- Coble, K., et al. 1999, ApJ, submitted, astro-ph/9902125
- de Oliveira-Costa A. et al., 1998, ApJ, 509, L77
- Ferreira, P. G. & Jaffe A. H. 1999, MNRAS, submitted astro-ph/9909250
- Goldin, A. B., et al. 1997, ApJ, 488, 161
- Griffin, M. 1986, Icarus, 65, 244
- Hildebrand R. 1985, Icarus, 64, 64
- Knox, 1999, Phys. Rev. D, submitted, astro-ph/9902046
- Kamionkowski, M. & Kosowsky, A., 1999, To appear in *Annu. Rev. Nucl. Part. Sci.*, astro-ph/9904108
- Masi, S. et al. 1998, Cryogenics, 38, 319
- Masi, S. et al. 1999, *BOOMERanG: a scanning telescope for 10 arcminutes resolution CMB maps*, in "Proceedings of the 3K Cosmology : EC-TMR Conference", Rome, Italy edited by L. Maiani, F. Melchiorri, and N.Vittorio AIP Conference Proceedings 237
- Masi S. et al. 1999, Cryogenics, 39, 217
- Mauskopf P., et al., Applied Optics, 36, 765, 1997
- Melchiorri A., et al. 1999, ApJ, submitted, astro-ph9911445
- Miller A.D. et al. 1999, ApJ, submitted, astro-ph/9906421
- Netterfield, C. B., et. al. 1997, ApJ, 474, 47
- Ostriker, J.P. & Steinhardt P. J. 1995, Nature 377, 600
- Schlegel D.J., Douglas P.F., Davis M. 1998, ApJ, 500, 525
- Torbet, E. et al. 1999, ApJ, 521, 79
- Turner, M.S. & White M. 1997, Phys. Rev. D., 56, R4439
- Ulich B.L. 1981, AJ, 86, 1619
- Wilson G.W. et al., preprint 1999, astro-ph/9902047
- Tegmark M. 1998, *CMB and LSS Power Spectrum Analysis*, in "Astrophysics and Algorithms: a DIMACS Workshop on Massive Astronomical Data Sets", 17
- Tegmark M. 1997, ApJ, 480, 87
- Wright, E. L., Smooth, G. F., Bennett, C. L., Lubin, P. M. 1994, ApJ, 436, 443
- Wright, E. 1996, astro-ph/9612006